

# Journal Pre-proof

Feasibility of chitosan crosslinked with genipin as biocoating for cellulose-based materials

Gonçalo Oliveira (Investigation) (Methodology) (Data curation) (Writing - original draft), Idalina Gonçalves (Conceptualization) (Investigation) (Methodology) (Writing - review and editing) (Validation) (Funding acquisition), Cláudia Nunes (Conceptualization) (Supervision) (Writing - review and editing), Paula Ferreira (Conceptualization) (Supervision) (Writing - review and editing), Manuel A. Coimbra (Supervision) (Writing - review and editing), Céline Martin (Supervision), Julien Bras (Supervision)



PII: S0144-8617(20)30603-2

DOI: <https://doi.org/10.1016/j.carbpol.2020.116429>

Reference: CARP 116429

To appear in: *Carbohydrate Polymers*

Received Date: 10 January 2020

Revised Date: 5 May 2020

Accepted Date: 6 May 2020

Please cite this article as: Oliveira G, Gonçalves I, Nunes C, Ferreira P, Coimbra MA, Martin C, Bras J, Feasibility of chitosan crosslinked with genipin as biocoating for cellulose-based materials, *Carbohydrate Polymers* (2020), doi: <https://doi.org/10.1016/j.carbpol.2020.116429>

This is a PDF file of an article that has undergone enhancements after acceptance, such as the addition of a cover page and metadata, and formatting for readability, but it is not yet the definitive version of record. This version will undergo additional copyediting, typesetting and review before it is published in its final form, but we are providing this version to give early visibility of the article. Please note that, during the production process, errors may be discovered which could affect the content, and all legal disclaimers that apply to the journal pertain.

© 2020 Published by Elsevier.

# Feasibility of chitosan crosslinked with genipin as biocoating for cellulose-based materials

Gonçalo Oliveira<sup>a</sup>, Idalina Gonçalves<sup>\*a</sup>, Cláudia Nunes<sup>a</sup>, Paula Ferreira<sup>b</sup>,  
Manuel A. Coimbra<sup>c</sup>, Céline Martin<sup>d</sup>, Julien Bras<sup>d</sup>

<sup>a</sup>CICECO - Aveiro Institute of Materials, Department of Chemistry, University of  
Aveiro, 3810-193 Aveiro, Portugal.

<sup>b</sup>CICECO - Aveiro Institute of Materials, Department of Materials and Ceramic  
Engineering, University of Aveiro, 3810-193 Aveiro, Portugal.

<sup>c</sup>QOPNA/LAQV, Department of Chemistry, University of Aveiro, 3810-193  
Aveiro, Portugal.

<sup>d</sup>University of Grenoble Alpes, LGP2, F-38000 Grenoble, France.

## Corresponding Author

\*Idalina Gonçalves ([idalina@ua.pt](mailto:idalina@ua.pt))

CICECO – Aveiro Institute of Materials, Complexo de Laboratórios Tecnológicos,  
Campus Universitário de Santiago, 3810-193 Aveiro, Portugal

Telephone: +351 234 370 200

Fax: +351 234 401 470

**Abstract**

Genipin crosslinking increases the acidic stability of chitosan-based materials, opening an opportunity to explore new applications. In this work, the viability of using chitosan-genipin solutions on cellulose-based materials coating was studied. Non-calendered paper and cardboard were used as raw materials. Different number of chitosan-genipin coating layers (1, 3, 6, 20, and 30) were applied and their influence on the materials mechanical, physicochemical, and barrier properties was studied. The small thickness and basis weight of non-calendered paper resulted in an inefficient adhesion of chitosan-genipin coating to the cellulose fibers. However, in cardboard, chitosan-genipin created a dense layer onto the cellulosic-fibers surface without impairing their mechanical properties. It conferred a greenish color, whose intensity increased with the layers number. The chitosan-genipin coating decreased the cardboard air and water vapor permeability up to 71% and 52%, respectively, and acted as a physical barrier for cardboard compounds leaching, being suitable for covering cellulose-based materials.

**Keywords**

Genipin crosslinking; Biobased coating; Paper-based materials; Barrier activity; Water vapor impermeability

## 1. Introduction

Cellulose-based materials have been widely used for packaging purposes due to their inherent biodegradability, thus minimizing the environmental impact caused by the petroleum-based plastics (Deshwal et al., 2019; Li et al., 2019). They have a porous crystalline structure constituted by microfibrils with long-chain cellulose molecules, regularly disrupted by amorphous regions (Khwaldia et al., 2010). However, the hydrophilic nature of cellulose and its porosity impair the materials' barrier properties, a fundamental parameter for the packaging industry. To overcome these issues, usually, cellulose-based materials are coated with synthetic polymers, *i.e.* petroleum-based polymers as polyethylene or polypropylene, which compromise their recyclability and biodegradability (Bordenave et al., 2007; Choi et al., 2002). Alternatively, biobased coatings derived from renewable and biodegradable polymers have been explored. Herein, polysaccharides have shown great affinity to the cellulose-based materials coating (Abdel Rehim et al., 2016; Chen et al., 2017; Kjellgren et al., 2006).

Chitosan, a partially deacetylated derivative of chitin composed by D-glucosamine and N-acetyl-D-glucosamine units linked by ( $\beta$ 1-4) glycosidic bonds (Rhim et al., 2007) has been applied on paper coating. Chitosan allows to decrease the cellulose matrix porosity and confers grease resistance to paper-based materials (Ham-Pichavant et al., 2005; Kjellgren et al., 2006). Due to its inherent antimicrobial and antioxidant properties, chitosan allows to produce active paper-based materials, offering a possibility of being used to preserve and extend the foodstuffs shelf-life (El-Samahy et al., 2017; Tang et al., 2016). Moreover, chitosan coating originates materials with better moisture and air

barrier properties than the uncoated paper (Bordenave et al., 2007; Reis et al., 2011). However, chitosan hydrophilicity compromises the barrier properties improvement for application on food packaging. To overcome these limitations, chitosan has been chemically modified, namely through esterification (Bordenave et al., 2010) or alkylation (Nicu et al., 2013), blended with lipidic compounds such as waxes (W. Zhang et al., 2014) or palmitic oil (Reis et al., 2011), and used on multi-layered coating systems (Despond et al., 2005; Kong et al., 2017). Crosslinking reactions have also been used to improve the moisture and gas barrier performance of chitosan-based films (Rivero et al., 2010) and hydrogels (D. Zhang et al., 2015).

Genipin, a natural molecule enzymatically obtained from *Gardenia jasminoides* fruits (Muzzarelli, 2009; Nunes et al., 2018), has been emerging as a favorable crosslinking agent due to its low cytotoxicity and ability to self-polymerization (Mekhail et al., 2014). Due to the genipin ability for reacting spontaneously with primary amine groups, it has been successfully used as an effective crosslinking agent for polymers containing amino groups, such as chitosan (Butler et al., 2003; Muzzarelli, 2009). Chitosan-genipin films have high stability in aqueous acidic media (Nunes et al., 2013), with application as a wine technological adjuvant (Nunes et al., 2016; Rocha et al., 2020) and as coating of magnesium alloy sheets for improved corrosion protection (Pozzo et al., 2018). Chitosan-genipin crosslinking has also been proposed for production of wound dressing materials with decreased hydrophilicity and increased flexibility (Hafezi et al., 2019; Liu et al., 2008) and for production of hydrogels with high elasticity and stability (Heimbuck et al., 2019; Moura et al., 2007). The combination of chitosan reticulated with genipin and cellulose has been performed for biomedical

applications through the production of delivery and encapsulation particles (Feng et al., 2013; Kaihara et al., 2011; Singh et al., 2017), hydrogels (Arikibe et al., 2019; Ghavimi, Lungren, Faulkner, et al., 2019; Ghavimi, Lungren, Stromsdorfer, et al., 2019) and 3D porous nanocomposite scaffolds (Naseri et al., 2016). Additionally, the genipin crosslinking helped immobilize nisin onto the surface of chitosan films reinforced with cellulose nanocrystals, leading to the increase of their water resistance, mechanical strength, and antimicrobial activity (Khan et al., 2014, 2016). The properties obtained by crosslinking chitosan and genipin opens an opportunity to explore other applications, such as the coating of cellulose-based materials. As the polymers reticulated with genipin are still biodegradable (You et al., 2014), a chitosan-genipin coating will not compromise the cellulose-based packaging sustainability.

In this work, it is hypothesized that the crosslinking of chitosan with genipin allows to form a coating to improve the barrier properties of cellulose-based materials. To test this hypothesis, non-calendered paper and cardboard were used as cases of study. The effect of chitosan-genipin coating layers number on mechanical, antioxidant, and barrier properties of cellulose-based materials was assessed. To ensure a suitable coating, the rheological profile of chitosan-genipin solutions was also studied.

## **2. Materials and Methods**

### **2.1 Materials**

Chitosan of high molecular weight (310 – 375 kg/mol) with a deacetylation degree of 75% and a viscosity of 800-2000 mPa.s (measured in a Brookfield viscosimeter using 1% wt. of chitosan in 1% w/V of acetic acid at 25 °C) was

supplied by Sigma–Aldrich. Genipin ( $\geq 98\%$  purity) was acquired from Challenge Bioproducts Co. (Taiwan, China). Acetic acid, sodium azide, calcium chloride, 2,2'-azino-bis(3-ethylbenzothiazoline-6-sulphonic acid) (ABTS) reagent and potassium persulfate were purchased from Sigma-Aldrich. Ethanol was obtained from Carlo Erba.

Two different cellulose-based materials were used to be coated: non-calendered paper (57 g/m<sup>2</sup> basis weight; 65  $\mu\text{m}$  average thickness), kindly provided by an industrial partner, and cardboard sheets (244 g/m<sup>2</sup> basis weight; 404  $\mu\text{m}$  average thickness) produced by Cascades La Rochette (France). Both materials have one side already coated and ready for printing purposes and another side still uncoated. Uncoated non-calendered paper and cardboard were used as control for comparison purposes.

## 2.2 Viscosity of chitosan-genipin solution

Chitosan (1% wt.) was prepared in 1% wt. of acetic acid solution at room temperature, overnight and with stirring. After filtration under vacuum, genipin (0.05% wt. of chitosan) prepared in ethanol was added to the chitosan solution. The ratio chitosan/genipin was chosen based on Nunes et al. (2013), adapting the gelation conditions by decreasing the time and varying the crosslinking temperature. Therefore, the influence of using different crosslinking temperatures (40, 50, and 60 °C) on viscosity of chitosan-genipin solution was assessed using 1000 s<sup>-1</sup> of shear rate for 120 min. These rheological experiments were performed using a modular compact MCR 302 rheometer (Anton Paar, France).



### **2.3 Cellulose-based materials coating**

Chitosan (1.2% wt.) was prepared in 1.2% wt. of acetic acid solution at room temperature, overnight and with stirring (Kjellgren et al., 2006). After filtration under vacuum, genipin (0.05% wt. of chitosan) (Nunes et al., 2013) prepared in ethanol was added into the chitosan solution and stirred for 30 minutes at 50 °C. Chitosan-genipin solution was applied on cellulose-based materials using a blade coater machine equipped with an infrared section (Endupap, France) and with a 0.2 mm Mayer bar at 6.46 cm/s with 300 g of load. Drying step was made with 2500 W of infrared radiation between the application of each coating layer. Various chitosan-genipin layers (1, 3, and 6 for non-calendered paper; 1, 3, 6, 20, and 30 for cardboard) were applied. Each coated material was pre-conditioned at 23 °C and 50% relative humidity for at least 24 h prior its characterization.

### **2.4 Cellulose-based materials characterization**

#### **2.4.1 Thickness and basis weight**

The thickness of each cellulose-based material was measured using an Adamel Lhomargy micrometer. The basis weight was calculated from the mass and thickness of stripes from all materials.

#### **2.4.2 Mechanical properties**

Paper-based strips of 130 x 15 mm were cut and the corresponding tensile properties were measured using a vertical extensometer (Instron 5965), following the standard NF Q03-004 (Desmaisons et al., 2017). Tensile tests were performed at 10 mm/min with a gauge length of 100 mm and six repeats were

performed per sample. Tensile strength, Young's modulus, and percentage of elongation at break of coated and uncoated materials were calculated. Each test was performed at conditioned atmosphere (23 °C and 50% RH).

The burst index (Adamel Lhomargy EC 0.5) was evaluated according to the standard ISO 2758/2759 (Lavoine et al., 2014). At least five measurements were done for each sample previously cut in square (100 × 100 mm).

The tear resistance was measured using a tear tester (Noviprofiber, Elmendorf pendulum 4000 mN, France) (Desmaisons et al., 2017). Samples of 65 x 50 mm were prepared, and the measurement corresponds to the force (mN) needed for tear propagation after a primer. For each cellulose-based material, two replicates were measured. Tear factor (mN m<sup>2</sup>/g) was determined from the division between the measured tear (mN) and the basis weight (g/m<sup>2</sup>) of each material.

### 2.4.3 Optical properties

The evaluation of color change was assessed by tristimulus colorimetry (CIELab). CIELab parameters, namely  $a^*$  (red/green),  $b^*$  (yellow/blue), and  $L^*$  (luminosity) components were determined using a CR-400 Chroma Meter (Luchese et al., 2018). The total color difference ( $\Delta E$ ) of the coated materials was calculated against the uncoated ones as follows:

$$\Delta E = [(L^* - 93.36)^2 + (a^* - (-0.65))^2 + (b^* - 7.53)^2]^{0.5} \quad (1)$$

where  $L^*$ ,  $a^*$ , and  $b^*$  are the CIELab parameters of each coated samples and 93.36, -0.65 and 7.53 are the CIELab parameters of the uncoated ones ( $L^*$ ,  $a^*$  and  $b^*$ , respectively).

#### **2.4.4 Scanning electron microscopy (SEM)**

The morphology of uncoated and chitosan-genipin coated materials was observed in a high-resolution field emission scanning electron microscope (Hitachi SU-70) operating at 4 kV and at an average working distance of 7 mm. Before examination, the samples were coated under vacuum with a thin layer of carbon using a Polaron sputter coater E5000. Images from top and cross-section views were obtained.

#### **2.4.5 Antioxidant activity**

The antioxidant activity of each uncoated and coated material was determined by an adaptation of the ABTS method described by Re et al. (1999). A solution of 7 mM ABTS was prepared in 2.45 mM potassium persulfate and kept in dark at room temperature for 16 h, allowing the ABTS<sup>•+</sup> formation. After, ABTS<sup>•+</sup> was diluted in ethanol (1:80) and the concentration of the solution was adjusted to obtain an absorbance value at 734 nm between 0.700 and 0.800, using a spectrophotometer (Jenway 6405 UV/Vis). Three replicates of each sample (10 × 10 mm) were placed on the top of a plastic cuvette with 1.5 mL ABTS<sup>•+</sup> solution. The cuvette was turned upside down in order to allow the reaction between the coated surface and the ABTS<sup>•+</sup> solution, under dark conditions at room temperature with orbital stirring (80 rpm). ABTS<sup>•+</sup> solution without any specimen was used as blank. The absorbance at 734 nm of the solutions was measured in triplicate after 2 and 7 days. The antioxidant activity was determined by the percentage of ABTS<sup>•+</sup> inhibition calculated as follows:

$$\text{Inhibition ratio (\%)} = 100 \times \frac{A_b - A_f}{A_b} \quad (2)$$

where  $A_b$  and  $A_f$  are the absorbance of blank (without cellulose-based material) and with cellulose-based material, respectively.

#### 2.4.6 Water contact angle

Static water contact angles (WCA) on the surface of each material were determined at room temperature using a contact angle measuring system (OCA 20, Dataphysics), fitted with an automatic image capture system (Dataphysics SCA20 M4) (Nunes et al., 2013). Each coated and uncoated material was cut in strips of 10 × 1 mm. A sessile 3  $\mu$ L drop of ultrapure water was dispensed on the sample surface using a microsyringe. After recording the droplet shape, the corresponding contact angle was calculated using the Laplace-Young method. At least eight droplet images were obtained along the sample length.

#### 2.4.7 Solubility in acid medium

For the determination of the materials solubility in acid aqueous medium, one square (4 cm<sup>2</sup>) of each material was immersed in 30 mL of water (pH 3.5) at room temperature with orbital agitation (80 rpm) for 7 days (Nunes et al., 2013). Afterwards, the materials were oven dried at 105 °C overnight and cooled down to room temperature inside a desiccator containing silica gel. The materials were weighed, and their solubility was given by the weight loss percentage calculated as follows:

$$\text{Weight loss (\%)} = 100 \times \frac{(m_b - m_a)}{m_b} \quad (3)$$

where  $m_b$  and  $m_a$  are the weight of dry sample before and after being immersed in acidic water, respectively. This determination was performed in triplicate.

#### 2.4.8 Air permeability

The air permeability of all materials was measured with a Mariotte vase, according to the standard ISO 5636 (Bideau et al., 2017). The measurements were performed on samples with an area of 10 cm<sup>2</sup>, under ambient air conditions with a vacuum of 2.1 kPa. A constant air depression was created by the flow of water from a glass container (Mariotte). The volume of water that flows in the catch tank was collected after a certain time and the average air permeability was then calculated from at least three measurements. The permeability index AFNOR (IAF) was obtained as follows:

$$IAF = \frac{V}{A \times t \times \Delta P} \quad (4)$$

where  $V$  is the volume of air in mm<sup>3</sup>,  $A$  is the area of the sample in m<sup>2</sup>,  $t$  is the time in seconds and  $\Delta P$  is the change in pressure in Pa.

#### 2.4.9 Water vapor transmission rate

Water vapor transmission rate (WVTR) of each uncoated and chitosan-genipin coated materials was evaluated using test dishes, following an adaptation of the TAPPI Standard T-448 om-09 method. Each material was cut in samples with 28 mm diameter, centered over the top of dishes containing a desiccant, anhydrous calcium chloride pre-dried at 200 °C for 16 h, and sealed to its open mouth using four screws symmetrically located around the dish circumference

and adhesive (Santos et al., 2006). After assembling, the apparatus was placed in a controlled humidity chamber maintained at 23 °C and 53% relative humidity using a saturated aqueous magnesium nitrate solution. Air was continuously circulated throughout the chamber with a fan (air velocity  $\approx$  160 m/min). Periodic weighing was performed to determine the rate of water vapor movement through the specimen into the desiccant. The dishes were weighted over the time until a constant rate of gain was attained. WVTR was calculated as follows:

$$WVTR \text{ (g/m}^2 \cdot \text{day)} = \frac{24 \times x}{A \times y} \quad (5)$$

where  $x$  is the gain in grams during the period  $y$ ,  $y$  is the time in hours for the gain of  $x$  and  $A$  is the exposed area of specimen ( $\text{m}^2$ ). Triplicates were tested for each cellulose-based material.

## 2.5 Statistical analysis

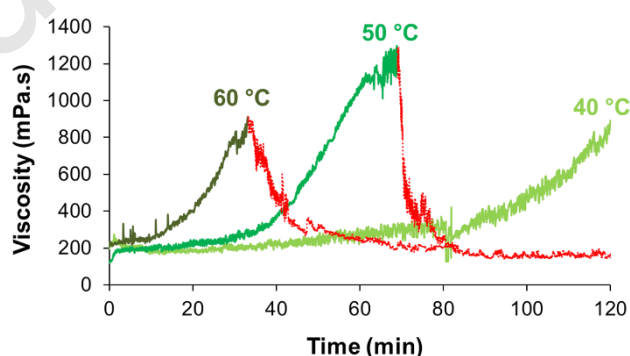
The data of thickness, mechanical properties, basis weight, CIELab parameters, antioxidant activity, water contact angle, acidic solubility, air permeability, and water vapor transmission rate were statistically evaluated using the  $t$ -Student test with a significance level of 95%.

## 3. Results and discussion

### 3.1 Influence of processing time and temperature on chitosan-genipin solutions viscosity

The performance of coated paper-based materials depends on the impregnation of the coating layer that is closely dependent on the coating solution viscosity applied on paper (Khwaldia et al., 2010). On the other hand, the chitosan-genipin crosslinking degree and consequent gelation process directly

depends on the reaction temperature that influences the activation energy required to induce the nucleophilic substitution of the ester group on the genipin molecule (Dimida et al., 2015). This phenomenon occurs through the secondary amide linkage between chitosan and genipin or by the oxygen radical-induced polymerization of genipin already linked to chitosan (Butler et al., 2003). Therefore, in this work, the viscous response of chitosan-genipin solutions at different temperatures (40; 50; and 60 °C) for 120 min with  $1000 \text{ s}^{-1}$  of shear rate stress was assessed. **Figure 1** shows that, at 40 °C, the viscosity of the chitosan-genipin solution slightly increased during the overall reaction time, reaching a viscosity value of around 890 mPa.s. By increasing the reaction temperature to 50 °C, during the initial 69 min of reaction, the viscosity increased up to around 1260 mPa.s, decreasing afterwards until reach a stationary baseline at around 150 mPa.s. At 60 °C, a similar viscosity profile was observed, *i.e.*, increased up to a maximum viscosity value and then decreased until reaching the baseline. However, the maximum viscosity value ( $\approx 910 \text{ mPa.s}$ ) was attained only after 33 min of reaction. For the experiments carried out at 50 and 60 °C, after the time allowed for reaction, the chitosan-genipin solutions formed a film. This explains the viscosity decrease after achieving the maximum viscosity value.



**Figure 1** - Viscosity profile of chitosan-genipin crosslinking performed at 40, 50, and 60 °C for 120 min with  $1000 \text{ s}^{-1}$  of shear rate. Red lines indicate the formation of a chitosan-genipin film.

The viscosity of chitosan-genipin solutions is directly related to the crosslinking degree between the two biomolecules, which is promoted by the increase of reaction temperature (Butler et al., 2003). Therefore, at 40 °C, the lowest viscosity values refer to the lower crosslinking chitosan-genipin degree obtained, when compared with the solutions crosslinked at 50 and 60 °C. Nevertheless, the highest viscosity value (1260 mPa.s) and, therefore, the high crosslink rate of chitosan-genipin solution was achieved when chitosan-genipin solution was processed at 50 °C and not at 60 °C. A lower temperature and higher time of reaction seemed to promote the extension of the reaction between genipin and chitosan, extending the crosslinking degree and, therefore, the increase of chitosan-genipin solution viscosity measured until the film was formed (Flores et al., 2019). For the coating of cellulose-based materials, 50 °C during 30 min were the selected crosslinking temperature and time conditions to achieve a crosslinking degree and solution viscosity that did not compromise the coating efficiency. In fact, high viscosity levels may give rise to blade bleeding and streaking, and some problems in maintaining the target coat weight (Khwaldia et al., 2010).

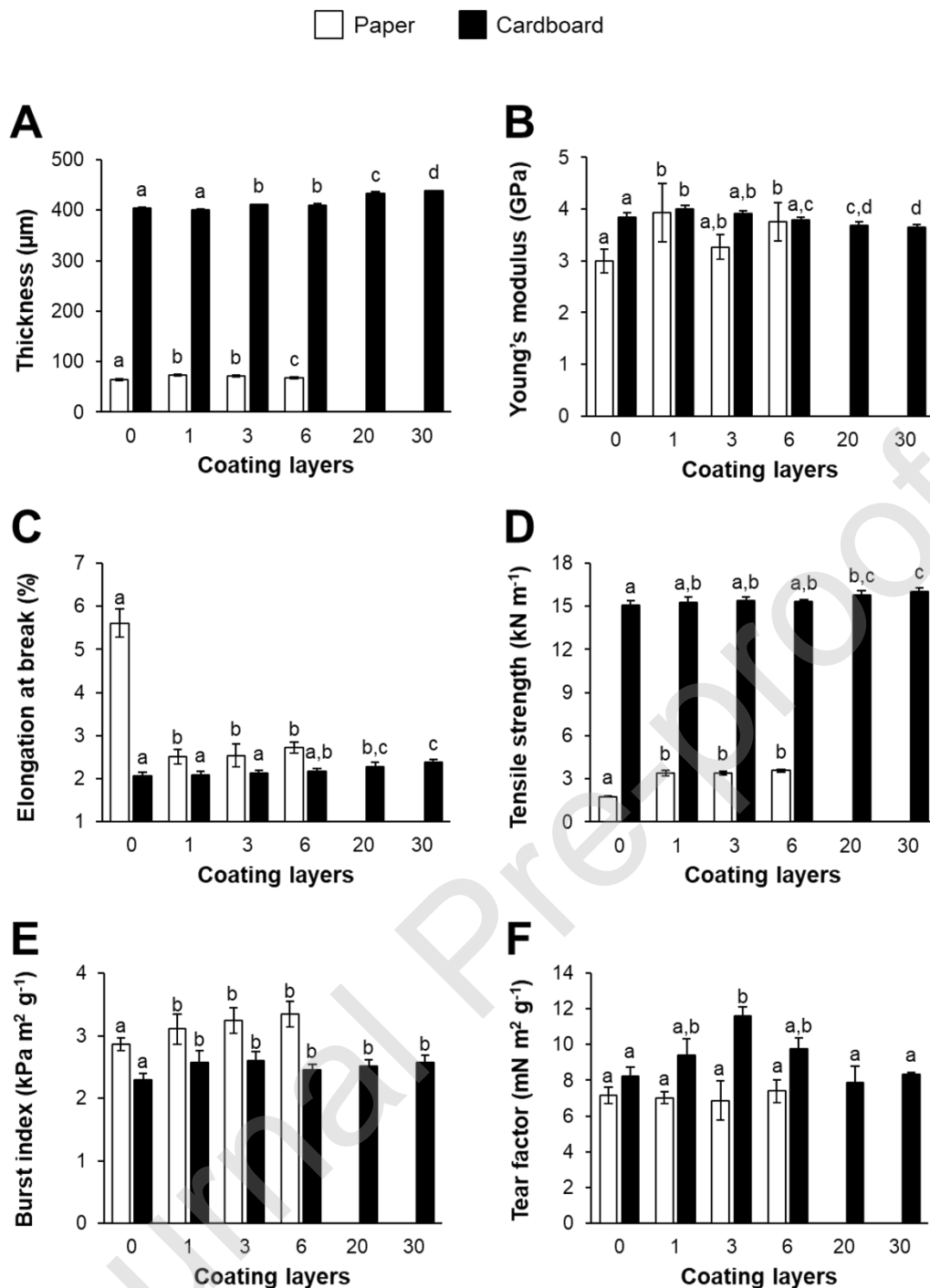
## **3.2 Cellulose-based materials characterization**

### **3.2.1 Influence of chitosan-genipin coating on thickness and mechanical properties**

The influence of chitosan-genipin coating layers on thickness and mechanical performance of cellulose-based materials (non-calendered paper and cardboard) was evaluated (**Figure 2**). For non-calendered paper, thickness



increased from 64.7  $\mu\text{m}$  (uncoated paper) to 72.2, 71.2, and 66.8  $\mu\text{m}$  (for 1, 3 and 6 chitosan-genipin coating layers, respectively) (**Figure 2A**). In addition, traction tests showed an increase in the Young's modulus values, from 2.99 GPa (uncoated paper) to 3.99, 3.27, and 3.71 GPa (for 1, 3, and 6 coating layers, respectively) (**Figure 2B**); a decrease in the elongation's values from 5.61% (uncoated paper) to 2.52%, 2.53%, and 2.72% (for 1, 3, and 6 coating layers, respectively) (**Figure 2C**); and an increase in the tensile strength's values from 1.75 kN/m (uncoated paper) to 3.41, 3.39 and 3.56 kN/m (for 1, 3, and 6 coating layers, respectively) (**Figure 2D**). The coated non-calendered paper showed an increase of the burst index from 2.86  $\text{kPa m}^2 \text{g}^{-1}$  to 3.10, 3.24 and 3.35  $\text{kPa m}^2 \text{g}^{-1}$  (for 1, 3, and 6 coating layers, respectively) (**Figure 2E**). On the contrary, tear measures for paper did not suffer any significant variation after being coated by chitosan-genipin (**Figure 2F**).



**Figure 2** – Thickness (A), Young's modulus (B), elongation at break (C), tensile strength (D), burst index (E), and tear factor (F) of uncoated and chitosan-genipin coated cellulose-based materials. Different letters for each sample represent values that are significantly ( $p < 0.05$ ) different.

For non-calendered paper coated with 1 and 3 chitosan-genipin layers, a thickness increase was observed. However, the thickness decreased between the 3 and 6 chitosan-genipin coating layers. This may be related with the cellulose

fibers hydration that affect their intrinsic properties, promoting their rearrangement (Kouris et al., 1958). This phenomenon, together with the pressure exerted by the bar coating weight, seem to have originated thinner materials, particularly when the starting samples had already a low thickness such as the one of the non-calendered paper (65  $\mu\text{m}$ ). The increase of Young's modulus values for chitosan-genipin coated non-calendered papers means that the coating makes paper's cellulose fibers more rigid, sustaining higher forces before deforming. Likewise, tensile strength increased equally for all coated papers, meaning that the coated papers supported higher forces than the uncoated cardboard before breaking. Nevertheless, papers coated with 3 chitosan-genipin layers showed an irregular Young's modulus value, which allowed to infer that the coating was not completely continuous along the cardboard surface. The rigidity increase was also proven by the significant decrease of the paper's elongation at break, *i.e.* the maximum length that films can stretch before breaking. Consequently, an increase of the paper's burst index with the chitosan-genipin coating was observed, indicating the need for a higher pressure to cause the rupture of the cellulose fibers. The deposition of chitosan-genipin onto the surface of the paper's cellulose fibers led to the formation of more rigid materials. Chitosan-genipin crosslinked films were already found to be more rigid than the pristine chitosan films (Mi et al., 2006; Nunes et al., 2013), which corroborates the mechanical performance observed for papers coated with chitosan-genipin.

For cardboard materials, the thickness remained constant for 1 chitosan-genipin coating layer, slightly increased from 403.9  $\mu\text{m}$  (uncoated cardboard) to 411.2 and 409.7  $\mu\text{m}$  (for 3 and 6 chitosan-genipin coating layers, respectively),

and considerable increased for 20 and 30 coating layers, reaching 432.8 and 438.0  $\mu\text{m}$ , respectively (**Figure 2A**). Young's modulus, elongation at break, and tensile strength values did not suffer any substantial changes up to the application of 20 chitosan-genipin coating layers (**Figures 2B, 2C, and 2D**). For 20 and 30 coating layers, a significant decrease in the Young's modulus values was observed (**Figure 2B**), as well as an increase in their elongation (**Figure 2C**) and tensile strength (**Figure 2D**). Burst index measures showed a small increase of this parameter for all coated cardboards (**Figure 2E**) and tear factor measures only increased for 3 chitosan-genipin coating layers, from 8.23  $\text{mN m}^2 \text{g}^{-1}$  to 11.62  $\text{mN m}^2 \text{g}^{-1}$  (**Figure 2F**). The mechanical changes verified for cardboards coated with 20 and 30 solution layers mean that the coating process could have changed the cellulose fibers organization, making them to hold low deforming forces and increased elasticity. Similar results were obtained by Bordenave et al. (2007), where chitosan coating ( $1.6 \text{ g/m}^2$ ) decreased the Young's modulus of Ahlstrom paper ( $48 \pm 1 \mu\text{m}$  thickness), acting as a plasticizer. On the other hand, the dense chitosan-genipin layer imparted traction resistance to the materials, given by the increase of their tensile strength and burst values. From a molecular point of view, chitosan-genipin acted as a reinforcing agent, increasing the cardboards mechanical resistance to break. The increase of tensile strength values was also observed on chitosan films after their crosslinking with genipin (Nunes et al., 2013). Moreover, the increase of tear factor for cardboard coated with 3 layers means that the force needed for tear propagation in this material was higher than any other, which corroborates the existence of some heterogeneity regarding the distribution of chitosan-genipin through the cardboard surface. Beyond the modification of the paper's pristine mechanical

properties after the chitosan-genipin coating, the non-calendered paper also became visually wrinkled when 6 chitosan-genipin coating layers were applied, which means that its fibrillar structure could not withstand the coating application. For these reasons, cardboard was selected for studying the influence of chitosan-genipin solution on morphological, optical, physicochemical, and barrier properties of cellulose-based materials, as it will be demonstrated in the following sections.

### 3.2.2 Influence of chitosan-genipin coating on cardboard structure

To evaluate the self-stratification of chitosan-genipin coating layers on the cardboard structure, basis weight and topography of each coated material were analyzed, using the uncoated cardboard as control. **Figure 2A** evidences the occurrence of a significant basis weight decrease between the pristine cardboard and the chitosan-genipin first layer. However, non-significant differences have been observed between the pristine and coated cardboards with 3 and 6 chitosan-genipin layers. This may be due to the hydration of the cellulose fibers in the first application, allowing a swelling of the surface. For the other coating layers, the deposition of chitosan along the applications seem to compensate this swelling effect, corroborating the observation of small thickness changes for cardboard materials up to 6 coating layers. By applying 20 and 30 chitosan-genipin layers onto the cardboard surface, an increase in 6.7% and 7.8% of its pristine thickness occurred, respectively. In accordance, only cardboards coated with 20 and 30 chitosan-genipin layers presented a significant increase in its basis weight, reaching a coat weight of 11 and 14 g/m<sup>2</sup>, respectively (**Table 1**). The increase of thickness and basis weight was achieved only when applying a high number of coating layers because the cardboard materials used are

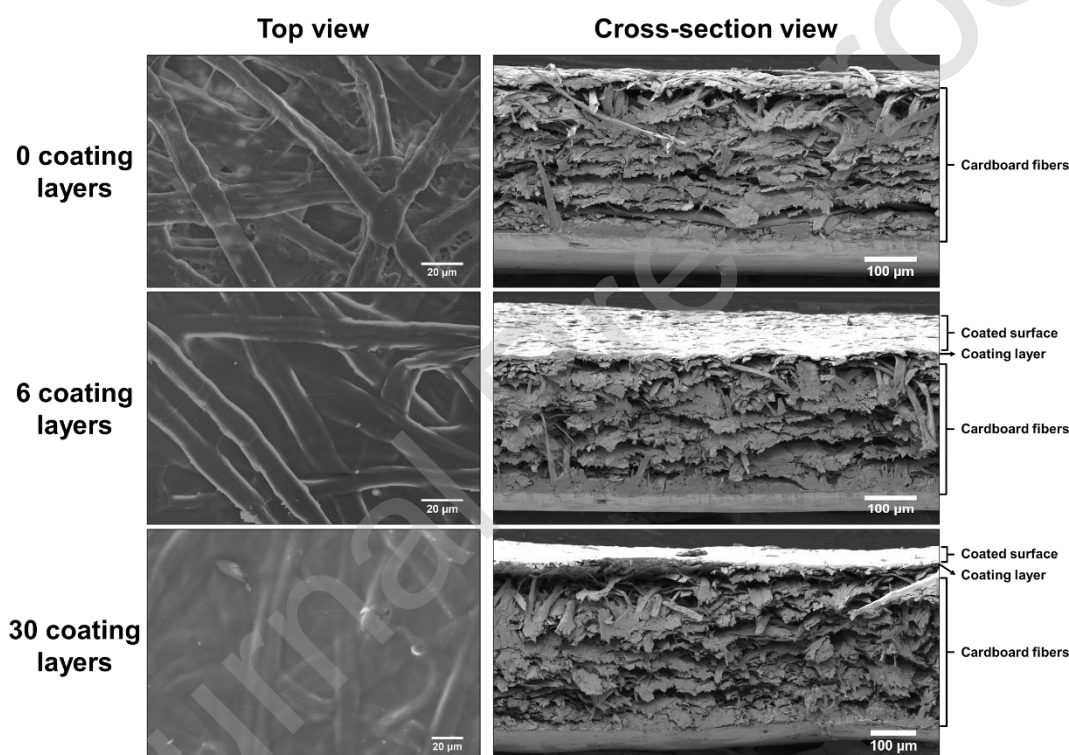
multilayered structures with improved mechanical properties and possessed significant basis weight (244 g/m<sup>2</sup>) and thickness (404 μm).

**Table 1** - Basis weight (g/m<sup>2</sup>) of uncoated and chitosan-genipin coated cellulose-based materials. Different letters represent values that are significantly ( $p < 0.05$ ) different.

Chitosan-genipin layers	Paper	Cardboard
0	57 ± 0 <sup>a</sup>	244 ± 2 <sup>a</sup>
1	58 ± 1 <sup>a</sup>	240 ± 3 <sup>b</sup>
3	57 ± 1 <sup>a</sup>	243 ± 2 <sup>a</sup>
6	57 ± 1 <sup>a</sup>	245 ± 3 <sup>a</sup>
20	-	255 ± 3 <sup>c</sup>
30	-	258 ± 2 <sup>c</sup>

The pristine cardboard fibers network and the morphology of cardboards coated with 6 and 30 layers of chitosan-genipin solution were analyzed by scanning electron microscopy (SEM) (**Figure 3**). For the uncoated cardboards, the top and cross-section SEM micrographs exhibited the typical porous structure of paper-based materials, with a developed network of cellulose fibers. Regarding cardboards coated with 6 layers, the fibers were still visible in the top view image, but the inter-fiber spaces were not so crisp. The cross-section view for this cardboard showed the formation of a thin layer above the fibers structure, corresponding to the chitosan-genipin coating. This observation is supported by the work of Fernandes et al. (2009), who studied the application of different layers of chitosan solution on paper sheets (75 g/m<sup>2</sup>). The authors concluded that the penetration of chitosan into the sheets occurred progressively with the first layers and after with 4 and 5 layers, a supplementary coating onto the paper was observed. Concerning cardboards coated with 30 layers, a great difference was observed. The top view micrographs showed a considerably reduction of the

cellulose fibers' sharpness, which means that more coating material was deposited above the cardboard surface. The blurred top-view image of the cardboard coated with 30 layers also supports the presence of a higher quantity of organic content. The cross-section view images confirmed the formation of a layer over the cardboard fibers which become thicker as the number of deposited layers increase, corroborating the great increase of thickness and coating weight of the cardboards. The chitosan-genipin film seems to be retained mainly at the cardboard surface as it cannot be observed at the inner layers of the cardboard.




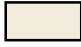




**Figure 3** - Scanning electron microscopy images of uncoated and coated cardboard materials with 6 and 30 chitosan-genipin layers.

### 3.2.3 Optical properties of chitosan-genipin coated cardboard

The visual appearance of the uncoated and chitosan-genipin coated materials shows that by coating with chitosan-genipin solution, the pristine yellowish coloration of cardboard changed to a greenish tone that is intensified

with the coating layers number. These optical modifications were monitored by the CIELab parameters measurement (**Table 2**). When compared to uncoated cardboard,  $L^*$  and  $a^*$  values decreased from 93.36 and -0.65 to 63.74 and -10.16, respectively, with the increasing of chitosan-genipin layers number, conferring a darker greenish coloration to the cardboard materials. Regarding the  $b^*$  parameter, it increased from 7.53 up to 11.22 for cardboards coated up to 6 coating layers, corresponding to an increase of the yellowish coloration, and then started decreasing up to 10.38 and 7.39 with 20 and 30 coating layers, respectively. The total color difference ( $\Delta E$ ) increased with chitosan-genipin layers number, being more accentuated in the 20 and 30 layers.

**Table 2** – CIELab values and total color difference ( $\Delta E$ ) of uncoated and chitosan-genipin coated cardboard materials. Different letters represent values that are significantly ( $p < 0.05$ ) different.

Chitosan-genipin layers	$L^*$	$a^*$	$b^*$	$\Delta E$	Visual appearance
0	93.36 ± 0.19 <sup>a</sup>	-0.65 ± 0.14 <sup>a</sup>	7.53 ± 0.22 <sup>a</sup>	-	
1	93.26 ± 0.23 <sup>a</sup>	-0.85 ± 0.13 <sup>b</sup>	8.23 ± 0.35 <sup>b</sup>	0.73	
3	91.97 ± 0.18 <sup>b</sup>	-0.73 ± 0.16 <sup>a</sup>	10.41 ± 0.33 <sup>c</sup>	3.21	
6	91.68 ± 0.56 <sup>b</sup>	-2.01 ± 0.19 <sup>c</sup>	11.22 ± 0.82 <sup>d</sup>	4.28	
20	74.64 ± 3.93 <sup>c</sup>	-7.51 ± 1.27 <sup>d</sup>	10.38 ± 1.61 <sup>c,d</sup>	20.14	
30	63.74 ± 4.24 <sup>d</sup>	-10.16 ± 1.11 <sup>e</sup>	7.39 ± 1.60 <sup>a,b</sup>	31.11	

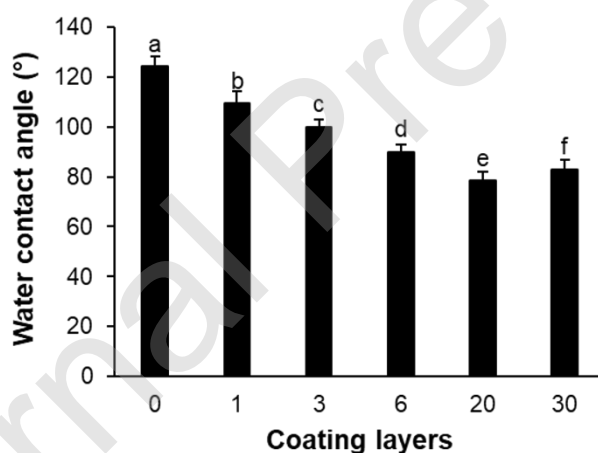
These phenomena derive from the chitosan-genipin crosslinking mechanism. Indeed, when added to a chitosan solution, genipin reacts through a nucleophilic attack with the primary amine groups present on chitosan structure, forming an intermediate aldehyde group that spontaneously reacts with the just formed secondary amine, and gives rise to a heterocyclic compound possessing a conjugated double bonding system that, depending on the crosslinking degree,



varies from light green to a dark blue coloration (Butler et al., 2003). Accordingly, the yellowish coloration observed for the chitosan-genipin solution immediately after its preparation (**Figure S1**) became increasingly greenish during the coating process.

### 3.2.4 Wettability of chitosan-genipin coated cardboard

The measures of the water contact angle (WCA) between the cardboards surface and a drop of ultra-pure water showed a decrease of this parameter with the chitosan-genipin coating (**Figure 4**). WCA decreased progressively from 124° (uncoated cardboards) to 109°, 100°, 90°, 78° and 83° (for 1, 3, 6, 20 and 30 chitosan-genipin coating layers, respectively).



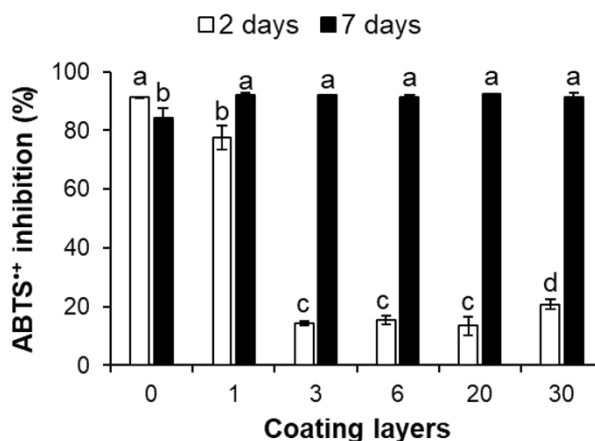
**Figure 4** – Water contact angle of uncoated and chitosan-genipin coated cardboard materials. Different letters represent values that are significantly ( $p < 0.05$ ) different.

The hydrophobic behavior of uncoated cellulose fibers should be due to the sizing process, where there is incorporation in cardboard's formulation of hydrophobic compounds such as waxes, fatty acid derivatives and resins (Tansley et al., 1995). On the other hand, the chitosan-genipin coating materials

became more hydrophilic due to the inherent hydrophilic character of chitosan. Despite of this WCA decrease, the lower WCA values (78° and 83°) obtained for cardboards coated with 20 and 30 chitosan-genipin layers, respectively, are close to the reference value (90°) to be considered as a hydrophobic material. Also, the pristine structure of cardboard coated materials was maintained even after being immersed in acid aqueous medium (**Figure S2**), without compromising their further application. This behavior may be related to the hydrogen bonding established between chitosan-genipin coating and the cellulose fibers (Wu et al., 2004), similarly to the hydrogen bonding that occurs between the ( $\beta$ 1 $\rightarrow$ 4)-Glc residues in cellulose fibrils and ( $\beta$ 1 $\rightarrow$ 4)-GlcN residues in chitosan. Accordingly, increased interaction between chitosan and cellulose when using 1% of a high molecular weight chitosan solution to coat paper-based materials has been observed by Tanpichai et al. (2019). In addition, the establishment of interactions between chitosan-genipin and cellulose could have changed the cellulose fibers organization, leading to the traction resistance increase of non-calendered and cardboard coated materials, as shown by the mechanical properties.

### **3.2.5 Antioxidant activity of chitosan-genipin coated cardboard**

Chitosan-genipin films have shown to inhibit microbial growth in wines while preserving their antioxidant activity (Nunes et al., 2016). To evaluate the possible antioxidant activity conferred by the chitosan-genipin coating, the ABTS<sup>•+</sup> inhibition promoted by all the cardboard materials (coated and uncoated) was determined after 2 and 7 days of exposure to the cationic radical solution (**Figure 5**).



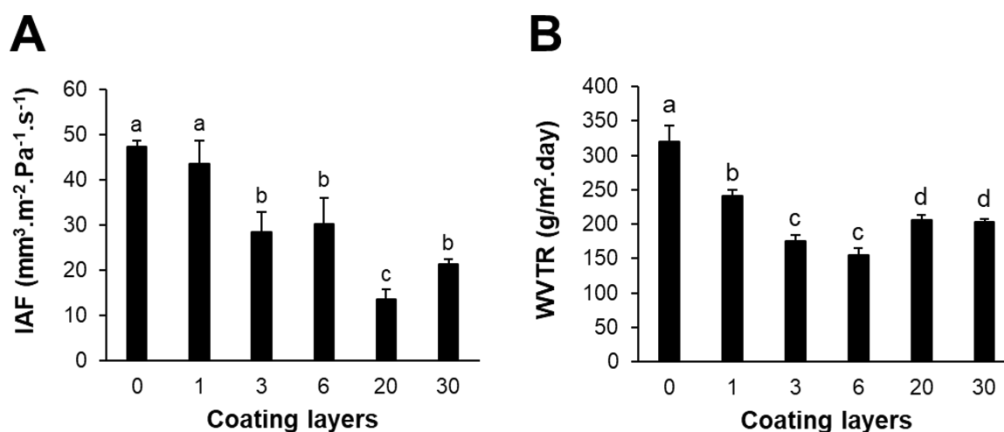
**Figure 5** - Antioxidant activity (by ABTS<sup>•+</sup> inhibition) of uncoated and chitosan-genipin coated cardboard materials after 2 and 7 days of incubation. Different letters represent values that are significantly ( $p < 0.05$ ) different.

For 2 days of incubation, a higher inhibition of the ABTS<sup>•+</sup> was obtained for uncoated cardboards ( $\approx 91.4\%$ ) and cardboards coated with just 1 coating layer ( $\approx 77.5\%$ ). This phenomenon may be due to the presence of some antioxidant compounds that are added to the cardboard's formulation during the sizing process, a procedure that have as main objective the improvement of the water resistance properties. Additives named "surface-active compounds" as dispersants and emulsifiers (conventional lignin, lignincarboxylate, carboxymethyl cellulose, ethylene oxide adducts of alkylphenols, fatty amines, fatty alcohols, fatty acid ester of polyvalent alcohols, substituted benzimidazoles or condensation products of formaldehyde and aromatic sulfonic acids) and as sulphate surfactants (diethanolamine, sodium lauryl or ethoxylated lauryl sulphates) are examples of possible sizing additives that may confer antioxidant activity to the cardboard materials (Bernheim et al., 1985). Comparing with uncoated cardboards, the addition of more coating layers decreased the antioxidant activity of cardboard materials from 91.4% to 14.3%, 15.3%, 13.4% and 20.8% (for 3, 6, 20, and 30 chitosan-genipin coating layers, respectively).

Here, chitosan-genipin coating may act as a physical barrier, inhibiting the interaction between the antioxidant compounds of cardboard formulations and the ABTS<sup>•+</sup> solution. Nevertheless, a significant increase of the ABTS<sup>•+</sup> inhibition was observed when 30 coating layers were applied onto the cardboard surface, meaning that, despite of the physical barrier, the chitosan-genipin coating contributed to the antioxidant activity increase. For 7 days of incubation, all cardboard coated materials reached the total inhibition of the ABTS<sup>•+</sup> ( $\approx 90\%$ ). This means that the coating barrier effect against the cardboard's sizing active compounds was overcome and the cardboard active compounds, together with the chitosan-genipin molecules, should have contributed to increase the materials antioxidant activity. This inhibition ( $\approx 90\%$ ) was higher than the ABTS<sup>•+</sup> inhibition of chitosan-genipin crosslinked films after the same 7 days of incubation, which was around 30% (Gonçalves et al., 2017) due to the active contribution of the sizing additives that were present in the cardboard formulation, enhancing the active potential of this cardboard after a longer period of time.

### **3.2.6 Barrier properties of chitosan-genipin coated cardboard**

Chitosan-genipin coating altered the air and water vapor permeabilities of pristine cardboard materials (**Figure 6**).



**Figure 6** – Air and water vapor permeability of uncoated and chitosan-genipin coated cardboard materials. Different letters represent values that are significantly ( $p < 0.05$ ) different.

The index AFNOR (IAF) decreased from 47.4 mm<sup>3</sup> m<sup>-2</sup> Pa<sup>-1</sup> s<sup>-1</sup> (uncoated cardboards) to 28.5, 30.3, 13.6, and 21.3 mm<sup>3</sup> m<sup>-2</sup> Pa<sup>-1</sup> s<sup>-1</sup> (for 3, 6, 20, and 30 chitosan-genipin coating layers, respectively) (**Figure 6A**). The decrease of this parameter means that the coating made cardboards less permeable to the air. For cardboards coated with 20 coating layers, air permeability reached a maximum decrease, which means that less air was able to get through this material. The permeability increase observed from 20 to 30 coating layers means that the permeability decrease verified with the coating application was not directly proportional to the number of coating layers applied onto the cardboard surface. This evidence was also shown by the IAF non-significant difference values obtained for 3 and 6 coated cardboards, implying that the application of the chitosan-genipin coating was not completely continuous through the cardboard surface. This heterogeneity is in accordance with the barrier properties results. The obtained barrier properties results are in accordance with Reis et al. (2011), where the resistance to air of Kraft paper (200 g/m<sup>2</sup>) was improved through the application of a chitosan coating with 2.6 and 3.5 g/m<sup>2</sup> of coat weight, showing the chitosan ability to improve the air resistance of the coated materials.

Chitosan coating also decreased progressively the air permeability of *Eucalyptus globulus*-based paper sheets (74 g/m<sup>2</sup> of basis weight and 100 µm of average thickness) by applying 1 to 5 chitosan coating layers (coat weight varied from 1.5 to 4.6 g/m<sup>2</sup>) (Fernandes et al., 2010). The air permeability of cellulose-based materials strongly depends on their porosity (Kjellgren et al., 2006). Since chitosan-genipin cannot be observed at the inner layers of the cardboard (**Section 3.2.2**), the formation of a dense layer of chitosan reticulated with genipin above the cellulosic surface seems to be fundamental to the decrease of the air permeability.

Chitosan-genipin coating decreased progressively the water vapor transmission rate (WVTR) values from 320 g/m<sup>2</sup>.day (uncoated cardboards) to 155 g/m<sup>2</sup>.day (cardboards coated with 6 chitosan-genipin layers) (**Figure 6B**). For 20 and 30 coating layers, WVTR also decreased when compared with uncoated materials, but not so drastically as in cardboards coated with 6 coating layers, reaching 206 and 203 g/m<sup>2</sup>.day for cardboards coated with 20 and 30 layers, respectively. All these values were significantly lower than the ones achieved by Reis et al. (2011), that coated Kraft paper with a bar equipment and obtained approximately 606 g/m<sup>2</sup>.day using a 4% chitosan solution and a coat weight of 3.5 g/m<sup>2</sup>. Unlike Kraft paper, cardboards are highly compacted multilayered structures with less porosity due to the vast presence of cellulose fibers, which make these materials less susceptible to the passage of water molecules through their structure. The decrease of WVTR of around 52% for 6 coating layers was due to the formation of a dense layer of chitosan-genipin above the cardboard's cellulosic fibers, making even more difficult the passage of water molecules. The slightly increase of WVTR for cardboards coated with 20

and 30 layers, when compared with cardboard coated with 6 layers, can be explained by the accumulation of chitosan-genipin on the top of the cardboard surface, as proven by thickness results (**Figure 2A**), allowing a high hydrogen bonding between chitosan-genipin and water molecules, corroborating with the wettability data (**Figure 4**). Therefore, 6 chitosan-genipin layers reveal to be the most suitable to enhance the moisture barrier properties of cardboards. Furthermore, the genipin crosslinking strategy made it possible to use a low amount of chitosan (1.2% wt.) in the coating solution, obtaining a WVTR decrease (2.1-fold) equal or higher than those obtained when 2, 3, and 4% wt. of chitosan were used to coat paper-based materials (Bordenave et al., 2007; Fernandes et al., 2010; Reis et al., 2011).

#### **4. Conclusion**

Chitosan-genipin coating originated greenish cardboards with high traction resistance and acted as a physical barrier for cardboard constituents after a short period of time. The higher amount of chitosan-genipin onto the cardboard surface led to an increase of the cardboard antioxidant activity. The crosslinking of chitosan with genipin allowed the use of a low amount of chitosan in the coating solution, creating a dense layer onto the cardboards surface, and significantly decreasing their water vapor and air permeabilities. Chitosan-genipin solution revealed to be a promising active biobased coating for cellulose-based materials, which may be able to expand their use on active food packaging. The air and water vapor barrier increase can contribute to extend the foodstuffs shelf-life, by minimizing their deterioration reactions over the storage time.

**Credit author statement**

**Gonçalo Oliveira:** Investigation; Methodology; Data curation; Writing- Original draft preparation

**Idalina Gonçalves:** Conceptualization; Investigation; Methodology; Writing - review & editing; Validation; Funding acquisition

**Cláudia Nunes:** Conceptualization; Supervision; Writing - review & editing

**Paula Ferreira:** Conceptualization; Supervision; Writing - review & editing

**Manuel A. Coimbra:** Supervision; Writing - review & editing

**Céline Martin:** Supervision

**Julien Bras:** Supervision

**Acknowledgments**

This work was developed within the scope of the projects QOPNA (UID/QUI/00062/2019), LAQV-REQUIMTE (UIDB/50006/2020) and CICECO-Aveiro Institute of Materials (UIDB/50011/2020 & UIDP/50011/2020), financed by national funds through the FCT/MEC and when appropriate co-financed by FEDER under the PT2020 Partnership Agreement. GO and IG thank COST action FP1495 for two short-term scientific mission grants. FCT is also thanked for the Investigator FCT program (PF, IF/00300/2015), for the Individual Call to Scientific Employment Stimulus (IG, CEECIND/00430/2017), and for the grants ref. SFRH/BD/143191/2019 (GO), SFRH/BPD/104712/2014 (IG), and SFRH/BPD/100627/2014 (CN). CN also acknowledges her research contract (CDL-CTTRI-88-89-97-ARH/2018) which is funded by national funds (OE), through FCT – Fundação para a Ciência e a Tecnologia, I.P., in the scope of the



framework contract foreseen in numbers 4, 5 and 6 of the article 23, of the Law Decree 57/2016, of August 29, changed by Law 57/2017, of July 19.

## References

- Abdel Rehim, M. H., El-Samahy, M. A., Badawy, A. A., & Mohram, M. E. (2016). Photocatalytic activity and antimicrobial properties of paper sheets modified with TiO<sub>2</sub>/Sodium alginate nanocomposites. *Carbohydrate Polymers*, *148*, 194–199.
- Arikibe, J. E., Lata, R., Kuboyama, K., Ougizawa, T., & Rohindra, D. (2019). pH-Responsive Studies of Bacterial Cellulose /Chitosan Hydrogels Crosslinked with Genipin: Swelling and Drug Release Behaviour. *ChemistrySelect*, *4*(34), 9915–9926.
- Bernheim, M. D., Meindl, H. D., & Rohringer, P. (1985). Process for sizing paper or cardboard with anionic hydrophobic sizing agents and cationic retention agents. Retrieved from <https://patents.google.com/patent/EP0175647A1/en>
- Bideau, B., Bras, J., Adoui, N., Loranger, E., & Daneault, C. (2017). Polypyrrole/nanocellulose composite for food preservation: Barrier and antioxidant characterization. *Food Packaging and Shelf Life*, *12*, 1–8.
- Bordenave, N., Grelier, S., & Coma, V. (2010). Hydrophobization and Antimicrobial Activity of Chitosan and Paper-Based Packaging Material. *Biomacromolecules*, *11*(1), 88–96.
- Bordenave, N., Grelier, S., Pichavant, F., & Coma, V. (2007). Water and Moisture Susceptibility of Chitosan and Paper-Based Materials: Structure–Property Relationships. *Journal of Agricultural and Food Chemistry*, *55*(23), 9479–9488.

- Butler, M. F., Ng, Y.-F., & Pudney, P. D. A. (2003). Mechanism and kinetics of the crosslinking reaction between biopolymers containing primary amine groups and genipin. *Journal of Polymer Science Part A: Polymer Chemistry*, 41(24), 3941–3953.
- Chen, G., Zhu, P., Kuang, Y., Liu, Y., Lin, D., Peng, C., Wen, Z., & Fang, Z. (2017). Durable superhydrophobic paper enabled by surface sizing of starch-based composite films. *Applied Surface Science*, 409, 45–51.
- Choi, J. O., Jitsunari, F., Asakawa, F., Park, H. J., & Lee, D. S. (2002). Migration of surrogate contaminants in paper and paperboard into water through polyethylene coating layer. *Food Additives and Contaminants*, 19(12), 1200–1206.
- Deshwal, G. K., Panjagari, N. R., & Alam, T. (2019). An overview of paper and paper based food packaging materials: health safety and environmental concerns. *Journal of Food Science and Technology*, 56(10), 4391–4403.
- Desmaisons, J., Boutonnet, E., Rueff, M., Dufresne, A., & Bras, J. (2017). A new quality index for benchmarking of different cellulose nanofibrils. *Carbohydrate Polymers*, 174, 318–329.
- Despond, S., Espuche, E., Cartier, N., & Domard, A. (2005). Barrier properties of paper–chitosan and paper–chitosan–carnauba wax films. *Journal of Applied Polymer Science*, 98(2), 704–710.
- Dimida, S., Demitri, C., De Benedictis, V. M., Scalera, F., Gervaso, F., & Sannino, A. (2015). Genipin-cross-linked chitosan-based hydrogels: Reaction kinetics and structure-related characteristics. *Journal of Applied Polymer Science*, 132(28), 42256.
- El-Samahy, M. A., Mohamed, S. A. A., Abdel Rehim, M. H., & Mohram, M. E.

- (2017). Synthesis of hybrid paper sheets with enhanced air barrier and antimicrobial properties for food packaging. *Carbohydrate Polymers*, 168, 212–219.
- Feng, H., Zhang, L., & Zhu, C. (2013). Genipin crosslinked ethyl cellulose-chitosan complex microspheres for anti-tuberculosis delivery. *Colloids and Surfaces B: Biointerfaces*, 103, 530–537.
- Fernandes, S. C. M., Freire, C. S. R., Silvestre, A. J. D., Desbrières, J., Gandini, A., & Neto, C. P. (2010). Production of coated papers with improved properties by using a water-soluble chitosan derivative. *Industrial and Engineering Chemistry Research*, 49(14), 6432–6438.
- Fernandes, S. C. M., Freire, C. S. R., Silvestre, A. J. D., Neto, C. P., Gandini, A., Desbrières, J., Blanc, S., Ferreira, R. A. S., & Carlos, L. D. (2009). A study of the distribution of chitosan onto and within a paper sheet using a fluorescent chitosan derivative. *Carbohydrate Polymers*, 78(4), 760–766.
- Flores, E. E. E., Cardoso, F. D., Siqueira, L. B., Ricardi, N. C., Costa, T. H., Rodrigues, R. C., Klein, M. P., & Hertz, P. F. (2019). I Process *Biochemistry*, 84, 73–80.
- Ghavimi, S. A. A., Lungren, E. S., Faulkner, T. J., Josselet, M. A., Wu, Y., Sun, Y., Pfeiffer, F. M., Goldstein, C. L., ... Ulery, B. D. (2019). Inductive co-crosslinking of cellulose nanocrystal/chitosan hydrogels for the treatment of vertebral compression fractures. *International Journal of Biological Macromolecules*, 130, 88–98.
- Ghavimi, S. A. A., Lungren, E. S., Stromsdorfer, J. L., Darkow, B. T., Nguyen, J. A., Sun, Y., Pfeiffer, F. M., Goldstein, C. L., ... Ulery, B. D. (2019). Effect of Dibasic Calcium Phosphate Incorporation on Cellulose

- Nanocrystal/Chitosan Hydrogel Properties for the Treatment of Vertebral Compression Fractures. *AAPS Journal*, 21(3), 1–12.
- Gonçalves, I., Nunes, C., Mendes, S., Martins, L. O., Ferreira, P., & Coimbra, M. A. (2017). CotA laccase-ABTS/hydrogen peroxide system: An efficient approach to produce active and decolorized chitosan-genipin films. *Carbohydrate Polymers*, 175, 628–635.
- Hafezi, F., Scoutaris, N., Douroumis, D., & Boateng, J. (2019). 3D printed chitosan dressing crosslinked with genipin for potential healing of chronic wounds. *International Journal of Pharmaceutics*, 560, 406–415.
- Ham-Pichavant, F., Sèbe, G., Pardon, P., & Coma, V. (2005). Fat resistance properties of chitosan-based paper packaging for food applications. *Carbohydrate Polymers*, 61(3), 259–265.
- Heimbuck, A. M., Priddy-Arrington, T. R., Padgett, M. L., Llamas, C. B., Barnett, H. H., Bunnell, B. A., & Caldorera-Moore, M. E. (2019). Development of Responsive Chitosan-Genipin Hydrogels for the Treatment of Wounds. *ACS Applied Bio Materials*, 2(7), 2879–2888.
- Kaihara, S., Suzuki, Y., & Fujimoto, K. (2011). In situ synthesis of polysaccharide nanoparticles via polyion complex of carboxymethyl cellulose and chitosan. *Colloids and Surfaces B: Biointerfaces*, 85(2), 343–348.
- Khan, A., Gallah, H., Riedl, B., Bouchard, J., Safrany, A., & Lacroix, M. (2016). Genipin cross-linked antimicrobial nanocomposite films and gamma irradiation to prevent the surface growth of bacteria in fresh meats. *Innovative Food Science and Emerging Technologies*, 35, 96–102.
- Khan, A., Salmieri, S., Frascini, C., Bouchard, J., Riedl, B., & Lacroix, M. (2014). Genipin cross-linked nanocomposite films for the immobilization of

- antimicrobial agent. *ACS Applied Materials and Interfaces*, 6(17), 15232–15242.
- Khwaldia, K., Arab-Tehrany, E., & Desobry, S. (2010). Biopolymer Coatings on Paper Packaging Materials. *Comprehensive Reviews in Food Science and Food Safety*, 9(1), 82–91.
- Kjellgren, H., Gällstedt, M., Engström, G., & Järnström, L. (2006). Barrier and surface properties of chitosan-coated greaseproof paper. *Carbohydrate Polymers*, 65(4), 453–460.
- Kong, S., Bai, Y., Wang, L., Liu, X., & Wang, S. (2017). Assembled Chitosan-Nanocellulose Paper and Molecular Dynamics Simulation. *Journal of Biobased Materials and Bioenergy*, 11(6), 533–542.
- Kouris, M., Ruck, H., & Mason, S. G. (1958). The effect of water removal on the crystallinity of cellulose. *Canadian Journal of Chemistry*, 36(6), 931–948.
- Lavoine, N., Desloges, I., Khelifi, B., & Bras, J. (2014). Impact of different coating processes of microfibrillated cellulose on the mechanical and barrier properties of paper. *Journal of Materials Science*, 49(7), 2879–2893.
- Li, Z., Yang, X., Li, W., & Liu, H. (2019). Stimuli-responsive cellulose paper materials. *Carbohydrate Polymers*, 210, 350–363.
- Liu, B.-S., Yao, C.-H., & Fang, S.-S. (2008). Evaluation of a Non-Woven Fabric Coated with a Chitosan Bi-Layer Composite for Wound Dressing. *Macromolecular Bioscience*, 8(5), 432–440.
- Luchese, C. L., Garrido, T., Spada, J. C., Tessaro, I. C., & de la Caba, K. (2018). Development and characterization of cassava starch films incorporated with blueberry pomace. *International Journal of Biological Macromolecules*, 106, 834–839.

- Mekhail, M., Jahan, K., & Tabrizian, M. (2014). Genipin-crosslinked chitosan/poly-L-lysine gels promote fibroblast adhesion and proliferation. *Carbohydrate Polymers*, *108*, 91–98.
- Mi, F.-L., Huang, C.-T., Liang, H.-F., Chen, M.-C., Chiu, Y.-L., Chen, C.-H., & Sung, H.-W. (2006). Physicochemical, Antimicrobial, and Cytotoxic Characteristics of a Chitosan Film Cross-Linked by a Naturally Occurring Cross-Linking Agent, Aglycone Geniposidic Acid. *Journal of Agricultural and Food Chemistry*, *54*(9), 3290–3296.
- Moura, M. J., Figueiredo, M. M., & Gil, M. H. (2007). Rheological study of genipin cross-linked chitosan hydrogels. *Biomacromolecules*, *8*(12), 3823–3829.
- Muzzarelli, R. A. A. (2009). Genipin-crosslinked chitosan hydrogels as biomedical and pharmaceutical aids. *Carbohydrate Polymers*, *77*(1), 1–9.
- Naseri, N., Poirier, J. M., Girandon, L., Fröhlich, M., Oksman, K., & Mathew, A. P. (2016). 3-Dimensional porous nanocomposite scaffolds based on cellulose nanofibers for cartilage tissue engineering: Tailoring of porosity and mechanical performance. *RSC Advances*, *6*(8), 5999–6007.
- Nicu, R., Lupei, M., Balan, T., & Bobu, E. (2013). Alkyl-chitosan as paper coating material to improve water barrier properties. *Cellulose Chemistry and Technology*, *47*(7–8), 623–630.
- Nunes, C., Coimbra, M. A., & Ferreira, P. (2018). Tailoring Functional Chitosan-Based Composites for Food Applications. *The Chemical Record*, *18*(7–8), 1138–1149.
- Nunes, C., Maricato, É., Cunha, Â., Nunes, A., Silva, J. A. L. da, & Coimbra, M. A. (2013). Chitosan–caffeic acid–genipin films presenting enhanced antioxidant activity and stability in acidic media. *Carbohydrate Polymers*,

91(1), 236–243.

- Nunes, C., Maricato, É., Cunha, Â., Rocha, M. A. M., Santos, S., Ferreira, P., Silva, M. A., Rodrigues, A., Amado, O., Coimbra, J., Silva, D., Moreira, A., Mendo, S., da Silva, J.A.L., Pereira, E., Rocha, S.M., Coimbra, M. A. (2016). Chitosan-genipin film, a sustainable methodology for wine preservation. *Green Chemistry*, 18(19), 5331–5341.
- Re, R., Pellegrini, N., Proteggente, A., Pannala, A., Yang, M., & Rice-Evans, C. (1999). Antioxidant activity applying an improved ABTS radical cation decolorization assay. *Free Radical Biology and Medicine*, 26(9–10), 1231–1237.
- Reis, A. B., Yoshida, C. M., Reis, A. P. C., & Franco, T. T. (2011). Application of chitosan emulsion as a coating on Kraft paper. *Polymer International*, 60(6), 963–969.
- Rhim, J.-W., & Ng, P. K. W. (2007). Natural Biopolymer-Based Nanocomposite Films for Packaging Applications. *Critical Reviews in Food Science and Nutrition*, 47(4), 411–433.
- Rivero, S., García, M. A., & Pinotti, A. (2010). Crosslinking capacity of tannic acid in plasticized chitosan films. *Carbohydrate Polymers*, 82(2), 270–276.
- Rocha, M. A. M., Ferreira, P., Coimbra, M. A., & Nunes, C. (2020). Mechanism of iron ions sorption by chitosan-genipin films in acidic media. *Carbohydrate Polymers*, 236, 116026.
- Santos, C., Seabra, P., Veleirinho, B., Delgadillo, I., & Lopes da Silva, J. A. (2006). Acetylation and molecular mass effects on barrier and mechanical properties of shortfin squid chitosan membranes. *European Polymer Journal*, 42(12), 3277–3285.

- Singh, P., Medronho, B., Alves, L., da Silva, G. J., Miguel, M. G., & Lindman, B. (2017). Development of carboxymethyl cellulose-chitosan hybrid micro- and macroparticles for encapsulation of probiotic bacteria. *Carbohydrate Polymers*, *175*, 87–95.
- Tang, Y., Hu, X., Zhang, X., Guo, D., Zhang, J., & Kong, F. (2016). Chitosan/titanium dioxide nanocomposite coatings: Rheological behavior and surface application to cellulosic paper. *Carbohydrate Polymers*, *151*, 752–759.
- Tanpichai, S., Witayakran, S., Wootthikanokkhan, J., Srimarut, Y., Woraprayote, W., & Malila, Y. (2019). Mechanical and antibacterial properties of the chitosan coated cellulose paper for packaging applications: Effects of molecular weight types and concentrations of chitosan. *International Journal of Biological Macromolecules*.
- Tansley, A. C., & Ballantine, J. D. (1995). System for sizing paper and cardboard. Retrieved from <https://patents.google.com/patent/US5626719A/en>
- Wu, Y. B., Yu, S. H., Mi, F. L., Wu, C. W., Shyu, S. S., Peng, C. K., & Chao, A. C. (2004). Preparation and characterization on mechanical and antibacterial properties of chitsoan/cellulose blends. *Carbohydrate Polymers*, *57*(4), 435–440.
- Y. Pozzo, L. fr, da Conceição, T. F., Spinelli, A., Scharnagl, N., & Pires, A. T. N. (2018). Chitosan coatings crosslinked with genipin for corrosion protection of AZ31 magnesium alloy sheets. *Carbohydrate Polymers*, *181*, 71–77.
- You, R., Xu, Y., Liu, G., Liu, Y., Li, X., & Li, M. (2014). Regulating the degradation rate of silk fibroin films through changing the genipin crosslinking degree. *Polymer Degradation and Stability*, *109*, 226–232.



Zhang, D., Zhou, W., Wei, B., Wang, X., Tang, R., Nie, J., & Wang, J. (2015).

Carboxyl-modified poly(vinyl alcohol)-crosslinked chitosan hydrogel films for potential wound dressing. *Carbohydrate Polymers*, 125, 189–199.

Zhang, W., Xiao, H., & Qian, L. (2014). Beeswax–chitosan emulsion coated paper with enhanced water vapor barrier efficiency. *Applied Surface Science*, 300, 80–85.

Journal Pre-proof

## Figure Captions

**Figure 1** - Viscosity profile of chitosan-genipin crosslinking performed at 40, 50, and 60 °C for 120 min with 1000 s<sup>-1</sup> of shear rate. Red lines indicate the formation of a chitosan-genipin film.

**Figure 2** – Thickness (**A**), Young's modulus (**B**), elongation at break (**C**), tensile strength (**D**), burst index (**E**), and tear factor (**F**) of uncoated and chitosan-genipin coated cellulose-based materials. Different letters for each sample represent values that are significantly ( $p < 0.05$ ) different.

**Figure 3** – Scanning electron microscopy images of uncoated and coated cardboard materials with 6 and 30 chitosan-genipin layers.

**Figure 4** – Water contact angle of uncoated and chitosan-genipin coated cardboard materials. Different letters represent values that are significantly ( $p < 0.05$ ) different.

**Figure 5** - Antioxidant activity (by ABTS<sup>•+</sup> inhibition) of uncoated and chitosan-genipin coated cardboard materials after 2 and 7 days of incubation. Different letters represent values that are significantly ( $p < 0.05$ ) different.


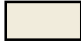

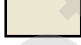

**Figure 6** – Air and water vapor permeability of uncoated and chitosan-genipin coated cardboard materials. Different letters represent values that are significantly ( $p < 0.05$ ) different.

## Tables

**Table 1** - Basis weight (g/m<sup>2</sup>) of uncoated and chitosan-genipin coated cellulose-based materials. Different letters represent values that are significantly ( $p < 0.05$ ) different.

Chitosan-genipin layers	Paper	Cardboard
0	57 ± 0 <sup>a</sup>	244 ± 2 <sup>a</sup>
1	58 ± 1 <sup>a</sup>	240 ± 3 <sup>b</sup>
3	57 ± 1 <sup>a</sup>	243 ± 2 <sup>a</sup>
6	57 ± 1 <sup>a</sup>	245 ± 3 <sup>a</sup>
20	-	255 ± 3 <sup>c</sup>
30	-	258 ± 2 <sup>c</sup>

**Table 2** – CIELab values and total color difference ( $\Delta E$ ) of uncoated and chitosan-genipin coated cardboard materials. Different letters represent values that are significantly ( $p < 0.05$ ) different.

Chitosan-genipin layers	$L^*$	$a^*$	$b^*$	$\Delta E$	Visual appearance
0	93.36 $\pm$ 0.19 <sup>a</sup>	-0.65 $\pm$ 0.14 <sup>a</sup>	7.53 $\pm$ 0.22 <sup>a</sup>	-	
1	93.26 $\pm$ 0.23 <sup>a</sup>	-0.85 $\pm$ 0.13 <sup>b</sup>	8.23 $\pm$ 0.35 <sup>b</sup>	0.73	
3	91.97 $\pm$ 0.18 <sup>b</sup>	-0.73 $\pm$ 0.16 <sup>a</sup>	10.41 $\pm$ 0.33 <sup>c</sup>	3.21	
6	91.68 $\pm$ 0.56 <sup>b</sup>	-2.01 $\pm$ 0.19 <sup>c</sup>	11.22 $\pm$ 0.82 <sup>d</sup>	4.28	
20	74.64 $\pm$ 3.93 <sup>c</sup>	-7.51 $\pm$ 1.27 <sup>d</sup>	10.38 $\pm$ 1.61 <sup>c,d</sup>	20.14	
30	63.74 $\pm$ 4.24 <sup>d</sup>	-10.16 $\pm$ 1.11 <sup>e</sup>	7.39 $\pm$ 1.60 <sup>a,b</sup>	31.11	